10TH INTERNATIONAL SYMPOSIUM ON PARTICLE IMAGE VELOCIMETRY - PIV13
Delft, The Netherlands, July 1-3, 2013

Bessel Beam Microscopy: Three Dimensional Particle Tracking with Super-Resolution

Craig Snoeyink[1], **Steve Wereley**[2]

[1] Department of Mechanical Engineering, Texas Tech University, Lubbock, USA craig.snoeyink@ttu.edu

[2] Department of Mechanical Engineering, Purdue University, West Lafayette, USA

ABSTRACT

Here we present an optical measurement technique and image analysis process capable of tracking particles in three dimensions with a single point of view. In addition to single view 3D-PTV, the optical system is capable of tracking individual particles even at particle-particle spacings that are closer than the diffraction limit of the base imaging system.

The measurement system, termed Bessel Beam Microscopy (BBM), functions as an attachment for a microscope that fits between the microscope base and camera. The addition of the BBM attachment transforms the point spread function (PSF) of the microscope allowing two unique functions: single image super-resolution imaging, and the extraction of three dimension location information of particles without calibration. The result is a fluid characterization tool with unique capabilities for micro and nano-scale velocimetry

1. INTRODUCTION

As the field of microfluidics has matured, the flows involved have continued to increase in complexity. Manufacturing ever smaller feature sizes has become increasingly easy. In addition, the range of forces available to manipulate particles and fluid flows has grown. What started with pressure or capillary driven flows has exploded into a range of dynamic and powerful forces such as dielectrophoresis, eletrothermophoresis, electrophoresis, acoustophoresis, and others.

Along with new abilities has come the need to measure and visualize the velocity fields within microfluidic devices. Micro Particle Image Velocimetery (μPIV), first introduced in 1998 quickly became the tool of choice for flow characterization in microfluidics [25, 20]. Instead of using a laser sheet, as is common in macroscale PIV, μPIV uses volume illumination with fluorescent particles. As a result, μPIV relies on the relatively thin focal depth of a microscope objective to restrict the imaged particles to the focal plane. The improvement of μPIV and its adaptation to a variety of fields, from biological to chemical and pharmaceutical measurements, is an ongoing process. Reviews of the state of the art for μPIV are published by Lindkin et. al. (2009) and Wereley and Meinhart (2010) [35, 17].

Micro-PIV is not with out its limitations. Since the technique uses volume illumination, particles that are not in the focal plane still contribute to the image. Flows with high velocity gradients can exhibit a significant error in what has been termed the depth of correlation problem [22]. Additionally the velocity field produced by micro-PIV is a two dimensional projection of a three dimensional velocity field. Both of these factors make μPIV ill suited for characterizing complex and three dimensional microfluidic flows. What is needed and what this paper addresses is a measurement method that can provide three dimensional flow characterization without errors due to velocity gradients.

In addition, the types of fluidic phenomena that are of interest to fluid mechanics researchers are expanding beyond the realm of traditional microfluidics. Researchers have used three dimensional particle tracking velocimetry to track the cytoplasm of cells as they swell due to osmosis, the paths of single walled nano-tubes as they enter and leave cells, and even observe neuron vesicle motion as the neuron is physically stressed [37, 2, 1, 12]. As the scale of these fluidic phenomena has shrunk so has the proximity of the particles of interest leading to problems as the length scales approach and pass the diffraction limit of the imaging system.

Bessel Beam Microscopy is a new imaging technique that is particularly well suited for particle tracking measurements in new and emerging fluidic measurements. The BBM system transforms the PSF of the microscope into a Bessel beam, the properties of which is related to to the depth providing a means by which to extract the three dimensional position of a particle from a single view image. In addition, the BBM system has been shown to have a spatial resolution that is up to 40% smaller than the base imaging system it is attached to. This makes the BBM system ideally suited for tracking particles in three dimensions and while closely spaced.

2. Experimental Setup

Bessel Beam Microscopy is based around the axicon, a unique optical element that has a conical surface [11, 19]. The axicon is most well known for its ability to closely approximate a Bessel Beam which can propagate long distances without diffracting or changing its intensity profile. Provided that the light beam incident on the axicon is paraxial, this non-diffracting beam can be used for imaging [28].

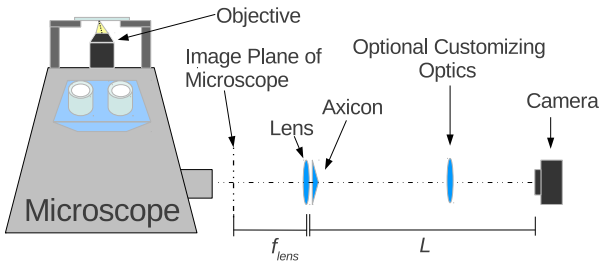

Figure 1: Schematic demonstrating arrangement of optical components in Bessel Beam Microscopy System.

To insure that the illumination is paraxial when incorporating the axicon into the light path of the microscope it is necessary to re-create the infinity space as shown in Fig. 1. To do this a single convex lens is placed its focal length away from the image plane of the microscope. In practice, a pair of lenses is typically used in order to achieve non-standard focal lengths such as 165 mm, the tube lens focal length of several popular microscope manufacturers. Immediately following this lens (or lenses) is the axicon which has very small surface angle, usually on the order of 1 degree.

Following the axicon the light beam is an approximation of a Bessel Beam and can propagate for long but limited distances without changes to the intensity profile. As a result there is no single plane in which the camera must be located as in a traditional imaging system. The camera can be placed any distance L from the axicon where L is an important variable affecting the behavior of the BBM system. Generally, increasing L will increase the lateral magnification of the system and the sensitivity of the system to changes in depth.

Finally, additional optics can be placed after the axicon to further customize the behavior of the BBM system. This allows the experimenter customize the spatial resolution, lateral magnification, and depth sensitivity of the system to the experiment at hand. The optical space in between the axicon and camera can be characterized by its system matrix, a 2x2 matrix with four components that are typically labeled A, B, C, and D [3]. Only two of these components are important for the BBM system, C and D. The behavior and effects of changing C and D are interrelated and will be explained more fully in later sections. However, in the context of the BBM system, C can be considered as the magnification component of the system matrix and D controls the width of the Bessel Beam central peak and the maximum value of C. For the simplified case of empty space between the axicon and camera the system matrix is such that C is equal to L and D is equal to 1.

3. Three Dimensional Particle Tracking Velocimetry

One important application of BBM is three dimensional Particle Tracking Velocimetry (3D-PTV). In 3D-PTV, a fluid flow is seeded with particles and the location of each individual particle is compared between two images to determine the velocity of that particle. The primary difficulty in performing PTV in three dimensions is in extracting three dimensional information on particle locations from images which are inherently two dimensional. Many successful solutions to this problem have been developed and can be broken down into two broad categories, multi-camera PTV and point spread function manipulation schemes. Point spread function manipulation schemes will be the focus of this section as this is the family of techniques that BBM belongs to.

3.1 Point Spread Function Manipulation

It is often not possible or practical to use multiple cameras or points of view. In this case it is possible to get information on the depth of a particle from the point spread function (PSF) of the imaging system. The PSF is essentially the image produced by a point source of light and is a strong function of distance from focal plane for most imaging systems. The way that this information is encoded in the image varies greatly. The simplest method measures the apparent diameter of the particle and correlates that to the depth of the particle. The farther from the focal plane a particle is the larger (more out of focus) it appears [38]. However, using the defocused particle image poses a few problems. It is not always obvious what features of the image to use or how to define them. Additionally, while it is possible to use this technique with very small particles [32], in practice one must use a dilute suspension of large particles in order to obtain clear particle outlines.

The PSF can also be modified in order to ease the process of determining the particle images radius. Digital Defocused micro Particle Tracking Velocimetry (DDuPTV), introduced in 1992 and applied to microscale flows in 2005, modifies the defocused image of the particle by putting an aperture with multiple pin holes in the optical path of the microscope [39, 36]. The technique is widely used and capable of diverse measurements such as measuring cardiac cell motion in a living embryo[18]. The addition of an aperture modifies the particle image, turning it into a set of dots for which the relative spacing is related to the depth of the particle. While this greatly simplifies the analysis of images, the aperture blocks a large portion of the light available from each particle reducing the contrast between the dots and background noise. A variation on this technique adds a color filter to each pin hole. The color coding of particle images eases the analysis of images allowing greater particle density [33].

An alternative method for modifying the particle image, called Astigmatism Particle Tracking Velocimetry (APTV), places a cylindrical lens in between the microscope and camera [7]. The cylindrical lens deforms the particle image into an ellipse where the major and minor axis lengths provide information on the depth of the particle. An advantage of this method is that, unlike other defocusing

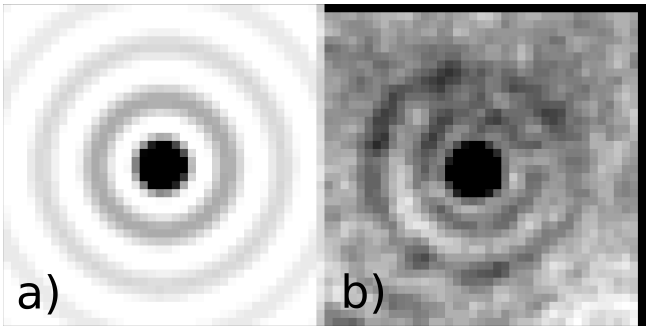

Figure 2: A) Simulated BBM point spread function (PSF) and B) Image of BBM PSF showing good agreement with theory. Both images have been inverted with adjusted contrast to enhance pattern visibility.

methods, APTV can self-calibrate using independent measures of the lengths of the two axis of the particle image ellipses [6]. However APTV, along with the other defocusing methods discussed, generally requires larger particles and dilute suspensions.

Finally, the use of coherent light allows one to directly reconstruct the position from the particle image. In Micro Digital holographic Particle Tracking Velocimetry (micro-DHPTV), the digital holograms are created by shining coherent light through a channel and analyzing the interference patterns produced by light scattered off seed particles as recorded by a digital camera [26, 15]. Since a single beam is used for both the reference and illumination wave alignment issues are significantly decreased and the measurement can be accomplished with equipment common to μPIV measurements [14, 4]. Micro-DHPTV is also uniquely flexible, it has no requirements on the tracer particles other than that they scatter light. As a result, micro-DHPTV can be used to follow un-tagged biological specimens[31]. While Micro-DHPTV has seen widespread application but suffers from several drawbacks [5], namely reduced resolution in the axial direction. The technique is, however, well suited to high particle densities, on the order of three thousand particles tracked simultaneously[27].

The three dimensional particle tracking system presented here is based on Bessel Beam Microscopy and is similar to the other PSF manipulation PTV schemes in that it only requires a single point of view to function. Using the optical setup described in Fig. 1, the PSF of the microscope is converted into a Bessel beam. This Bessel PSF is a strong function of the depth of the particle allowing for the extraction of depth information from the image of a particle.

One of the unique features of the BBM system is that the three dimensional PSF has a simple and closed analytical solution. This solution is based on the PSF of a single axicon illuminated by a paraxial point source, a point source located sufficiently far from the axicon and situated close enough to the optical axis that all light rays for small angles with the optical axis. Given these conditions, the PSF of the axicon has the following form:

$$I(r_c) \propto J_0^2(\beta r_c) \tag{1}$$

where where r_c is the radius from the particle pattern center, J_0 is a zero order Bessel function of the first kind, and β is the frequency of the Bessel function. As has been shown, the spatial frequency of the Bessel function is a function of the apparent Z position of the point source:

$$z_p \approx \frac{\beta z_i}{k\alpha(n-1)-\beta} \tag{2}$$

where where α is the angle of the axicon, n is the axicon's index of refraction, and z_i is the distance between the axicon and the imaging plane [28]. An example of the theoretical BBM PSF shown alongside an experimental image can be found in Fig. 2.

If the frequency of the Bessel function can be determined, then the apparent distance of the point source can be determined from Eqn. 2. Once the distance of the point source is known, the x and y location can be found from the center of the pattern[29].

Once the location of the point source image has been determined relative to the axicon, the actual location of the point source can be found by ray tracking backwards through the imaging system [29]. The key step in this process is finding the spatial frequency of the Bessel beam image. A robust and fast algorithm for spatial frequency determination is described in Snoeyink and Wereley (2013) that is centered around a cross-correlation optimization[29]. Ideal Bessel patterns of known frequency are cross-correlated with a Bessel pattern of unknown frequency. The magnitude of of the cross-correlation peak is maximized with the frequency of the Ideal Bessel pattern as the only variable. The spatial frequency that has the highest spatial frequency is the best estimate of the spatial frequency of the unknown image pattern.

The algorithm described in the Bessel Function Frequency section will always return a frequency. Thus, it becomes important to implement a heuristic that can determine valid particles from noise. The improved set of rules presented here is the result of an effort to move from an ad-hock to a physically reasoned heuristic. The result is greatly simplified and far more robust. It should be noted that the values listed below are such as to prevent the possibility of false positives. As a result, sub-optimal particles can also be filtered out despite still being accurate.

Once a potential particle pattern has been found, a two dimensional Gaussian is fit to the particle peak. The standard deviation from

this surface fit is a measure of the width of the central peak and a rough estimate of the spatial frequency of the Bessel pattern. A window is drawn around the potential pattern equal to 2.5 standard deviations. The standard deviation, maximum, and mean values of the pixels within this window are predictable if the pattern is a Bessel function. In particular the following configuration of these parameters should fall within the given range:

$$0.3 \leq \frac{\mu_{window} A_{window}}{\sigma_{window}} \leq 0.5 \tag{3}$$

where μ_{window} is the window average, A_{window} is the maximum value in the window, and σ_{window} is the standard deviation of pixel values in the window. If the pattern is not a Bessel function, then these values will fall outside of the predicted range. The bounds can be adjusted to change the selectivity of the filter.

After the frequency of the potential particle pattern has been determined via the cross-correlation optimization algorithm it can be compared to the initial estimate obtained from the two dimensional Gaussian fit. While some difference is to be expected, the two different methods should produce an estimate of the peak width that is within 30%. Again, this value can be adjusted to make the filter more or less permissive.

There are several advantages to using BBM for three dimensional particle tracking. In particular, the insensitivity of this technique towards particle size and brightness and lack of calibration are unique among 3D-PTV techniques that rely on the particle image. This provides an advantage in situations in which the size or brightness of the particles varies significantly or is not known ahead of time. Alternatively, this Interference-PTV is well suited to situations where non-uniformity in illumination can not be controlled for in the experiment.

3.2 Longitudinal Resolution

With three dimensional particle tracking measurements the longitudinal resolution is often much worse than the lateral or in plane resolution. For the BBM system we can get a measure of the resolution by deriving the sensitivity s which is defined as:

$$s \equiv \frac{dz_o}{d\beta} \tag{4}$$

By modeling the imaging system as a single convex lens of focal length f and numerical aperture NA immediately followed by an axicon it is possible to find an analytical expression for the sensitivity of the BBM system to changes in depth.

For this simplified system, the image depth of a particle near the focal plane of the lens is given by the well known thin lens equation:

$$z_i = \left(\frac{1}{f_{obj}} - \frac{1}{z_o} \right)^{-1} \tag{5}$$

where z_i is the location of the point source image, f_{obj} is the focal length of the lens, and z_o is the location of the point source. This can be combined with Eqn. 2 to relate the position of the point source in front of the lens to the spatial frequency of the resulting Bessel beam image. Solving for z_o, the position of the point source and taking the derivative with respect to β gives the following expression for the sensitivity:

$$\frac{dz_o}{d\beta} = -\frac{C f_{obj}^2 k\alpha (n-1)}{\left[\beta \left(C + f_{obj} D\right) - f_{obj} k\alpha (n-1)\right]^2} \tag{6}$$

This equation, while neglecting the effects of image noise, provides a useful tool for exploring the behavior of the longitudinal resolution in the BBM system. For example, from this equation it is clear that increasing the value of C increases the sensitive with respect to depth. Additionally, decreasing the focal length of the lens will also increase the sensitivity. Less obviously, it is also advantageous to increase D, as it increases the maximum allowable value of C. Finally, one can also decrease the surface angle of the axicon to increase the longitudinal sensitivity. Equation 6 can also provide a useful estimate of lateral resolution in measurement. Figure 3 shows the calculated path of a particle entrained in a micro-vortex caused by electrothermal flow. Using the effective focal length of 20x microscope objective with a NA of 0.45, an axicon surface angle of 1^o made of BK7 glass, and with a distance of 230 mm between the axicon and camera ($D = 1$ and $C = 230mm$) this equation estimates a resolution of about $4\mu m$, similar to the uncertainty in height previously determined experimentally for the same setup [29].

The particle trail shown in Fig. 3 is of a one micron fluorescent particle entrained in a micro-vortex. This microvortex is caused by a temperature gradient, from a focused laser, placed in between two planar electrodes[16]. In this case the planar electrodes are separated by a distance of $50\mu m$, a geometrical feature well reconstructed by the calculated velocity. Additionally, this measurement used only about 10% of the dynamic range, indicating a possible measurement depth of approximately $500\mu m$. A plot of the minimum resolvable depth as a function of particle depth for the experimental setup in Fig. 3 is shown in Fig. 4. For this experiment, the particle was in a region of $250\mu m$ to $300\mu m$ from the focal plane, indicating an uncertainty in the depth measurement of between 3 and 4 μm.

Perhaps more importantly, Eqn. 6 indicates that the longitudinal resolution of the BBM system is highly customizable. For example, when using a microscope only a few common objective magnifications are available. This would correspond to only few fixed f_{obj} in Eqn. 6. However, the effective focal length of the microscope objective can be modified by changing the focal length of the lens shown in Fig. 1. If the focal length of this lens is chosen equal to the focal length of the microscope tube lens then the effective focal length of the microscope objective is unchanged. If the focal length of this lens is chosen to be shorter then the tube lens focal length then there

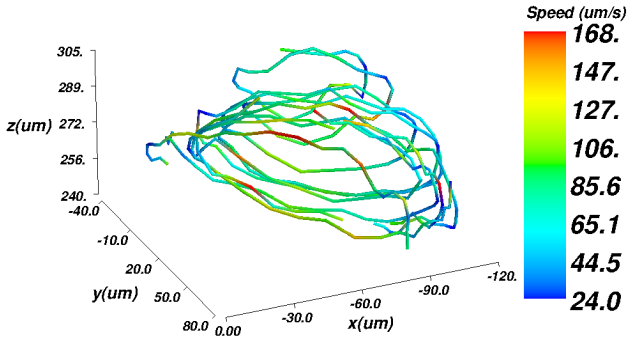

Figure 3: Trail plot of particle caught in electrothermal vortex, speed is indicated by color.

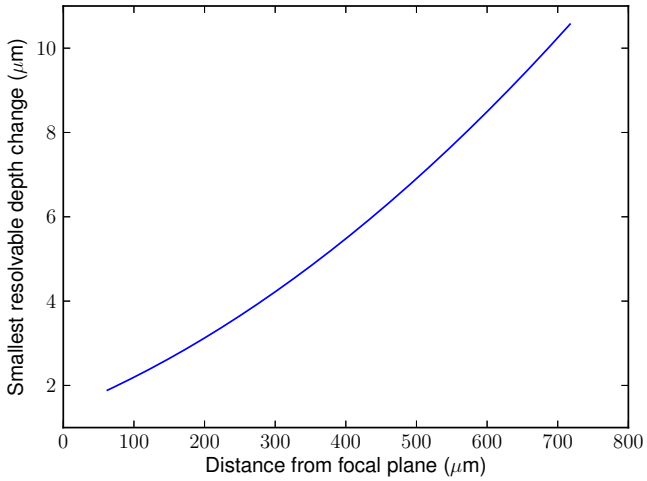

Figure 4: Estimated uncertainty plotted vs. particle depth for particle in Fig. 3

is an increase in the magnification of the microscope equal to the ratio of the two focal lengths (f_{tube}/f_{lens}). This also corresponds to a decrease in the effective focal length of the microscope objective.

Looking at a specific case with a 100x 1.45 NA oil immersion microscope objective with f_{lens} chosen to increase the magnification by 4 times and with an axicon with a surface angle of 1.0 degrees gives a longitudinal resolution on the order of 50 *nm*. This is competitive with other high resolution three dimensional particle tracking techniques but, as will be discussed in the next section, with the addition ability of tracking with sub-diffraction limit particle spacing. Further hypothetical gains can be made if axicons with super shallow surface angles are available. Given the same microscope objective but with an axicon with a surface angle of 0.125 degrees and a value of 0.06125 and 116 *mm* for the *D* and *C* components of the system matrix gives a longitudinal resolution on the order of 5 *nm*

4. Super-Resolution Particle Tracking

One difficulty in particle tracking is in dealing with objects that are closer together than the diffraction limit of the imaging system. This diffraction barrier limits the imaging resolution of conventional microscopes to 200*nm* to 300*nm* in the lateral dimension. This limit applies only for particles that are close together, isolated particles can be localized with precision limited only by the quality of the image [23, 13]. However, for particles located closer together than the diffraction limit localizing each particle accurately is more difficult. Recently, algorithms have been developed to estimate the locations of fluorescent emitters with overlapping PSF [10]. This algorithm uses a maximum-likelihood estimator to fit the intensity distribution of up to 5 partially overlapping emitters limiting its applicability to cases where particle voerlap is relatively unlikely.

The BBM system, in contrast, is capable of tracking an unlimited number of particles that are spaced as close as 0.6 times the diffraction limited resolution of the microscope [30]. This increased resolution is a result of the unique PSF of the BBM system, namely the Bessel beam. When the camera-axicon distance as shown in Fig. 1 is maximized, it is possible to show that the BBM system has a diffraction limited resolution that is approximately two thirds that of the base microscope.

This resolution increase is analogous to the resolution increases demonstrated by pupil plane filters [21, 24, 34]. Using a pupil plane filter increases the resolution by narrowing the central peak of the PSF with the side effect of increasing the intensity of side lobes like

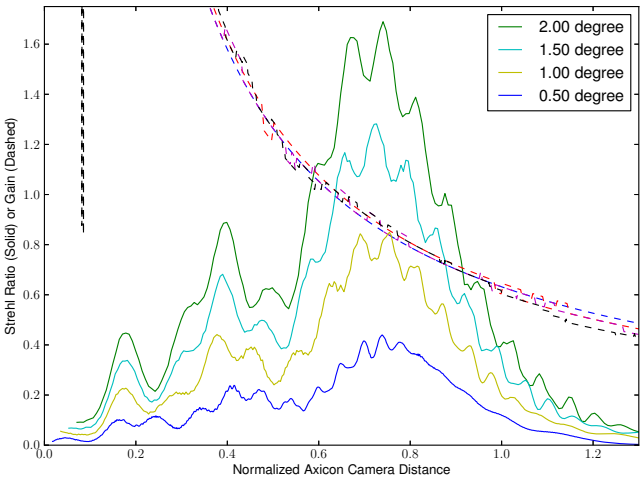

Figure 5: Plot of Strehl Ratio and Gain for BBM systems with different axicon surface angles as a function of normalized distance between axicon and camera.

those seen in Fig. 2 and decreasing the intensity of the central peak[24]. The resolution increase is typically reported as "Gain" which is the resolution of the filter system divided by the resolution of the base system. The intensity of the central peak is measured using the Strehl ratio, the intensity of the filter system divided by the intensity of the base imaging system. Recently, pupil plane filters with a continuously varying phase have been more successful at navigating the trade off between spatial resolution, intensity, and side-lobe strength achieving gains of 0.65 and a Strehl ratio of 0.28 [8, 9].

The goal then of any system that manipulates the PSF of the microscope to increase the resolution is to minimize the Gain while maximizing the Strehl ratio. A high Strehl ratio indicates a brighter image and a greater signal to noise ratio. Uniquely, the BBM system allows independent control of these two variables. Figure 5 shows a plot of the Gain and Strehl ratio for several BBM systems with varying axicon surface angles calculated from a diffraction simulation of a microscope with the BBM attachment.

The Gain and Strehl ratio of the BBM system are a function of both the distance between the axicon and camera, L in Fig. 1, and the surface angle of the axicon. However, when plotted against the normalized axicon-camera distance the Gain curves collapse to one that is only a function of the normalized distance. The Strehl ratio, however, increases with increasing axicon surface angle. Looking at a normalized axicon-camera distance of 1.0 provides a Gain of about 0.65, the theoretical maximum resolution increase of the BBM system. Interestingly, the BBM system with a surface angle of 1.5 degrees has a Strehl ratio of 0.4, an improvement over the best phase filter system.

The increase in Strehl ratio is a result of increasing the spatial frequency of the Bessel beam pattern, effectively shrinking it. While the width of the Bessel beam central peak can be decreased almost to the width of the wavelength of light, in practice there ceases to be a benefit once the width of the central peak becomes smaller than the width of a pixel. For a pixel size of $6\mu m$ this corresponds to an axicon surface angle of 4 *degrees*. At this surface angle the Strehl Ratio at maximum gain is approximately 0.5, nearly twice that of competing systems.

As a result, BBM represents a practical and simple super-resolution imaging system capable of acquiring super resolution images in a single acquisition. For this reason it is uniquely capable of tracking sub-diffraction spaced particles as a result of the larger Strehl ratio which indicates that there is more light available for imaging. This increases the frame rate and temporal resolution of the system opening up the possibility of dynamic measurements of sub-diffraction limit phenomena.

5. Conclusion

The BBM system is a unique imaging system that relies on an axicon to focus the image. This, along with the unique optical setup described here provides several advantages for particle tracking in fluids. In addition to not requiring calibration and being insensitive to changes in particle size or brightness, it is possible to calculate the uncertainty of the depth measurement. This allows the experimenter to customize the measurement depth and sensitivity to the particular experiment.

In addition, the BBM system is capable of acquiring single image super-resolution images. This give the unique ability to track particles even when the spacing falls below the diffraction limit of the base microscope. In addition, the BBM system is capable of a higher Strehl ratio than competing systems. This gives brighter images and shorter camera exposure times opening up the possibility of capturing time resolved sub-diffraction limit particle and fluid dynamics.

REFERENCES

[1] Wylie W Ahmed, Brian J Williams, Aaron M Silver, and Taher A Saif. Measuring nonequilibrium vesicle dynamics in neurons under tension. *Lab on a chip*, 13(4):570–8, January 2013.

[2] Alvaro Barroso, Mike Woerdemann, Angelika Vollmer, Gert von Bally, Björn Kemper, and Cornelia Denz. Three-Dimensional Exploration and Mechano-Biophysical Analysis of the Inner Structure of Living Cells. *Small (Weinheim an der Bergstrasse, Germany)*, November 2012.

[3] Max Born and Emil Wolf. *Principles of optics*. Cambridge University Press, New York, seventh (e edition, 1999.

[4] Yong-Seok Choi, Kyung-Won Seo, Myong-Hwan Sohn, and Sang-Joon Lee. Advances in digital holographic micro-PTV for analyzing microscale flows. *Optics and Lasers in Engineering*, 50(1):39–45, January 2012.

[5] C. Cierpka and C. J. Kähler. Particle imaging techniques for volumetric three-component (3D3C) velocity measurements in microfluidics. *Journal of Visualization*, 15(1):1–31, October 2011.

[6] C Cierpka, M Rossi, R Segura, and C J Kähler. On the calibration of astigmatism particle tracking velocimetry for microflows. *Measurement Science and Technology*, 22(1):15401, January 2011.

[7] C Cierpka, R Segura, R Hain, and C J Kähler. A simple single camera 3C3D velocity measurement technique without errors due to depth of correlation and spatial averaging for microfluidics. *Measurement Science and Technology*, 21(4):45401, 2010.

[8] Daniel M de Juana, José E Oti, Vidal F Canales, and Manuel P Cagigal. Design of superresolving continuous phase filters. *Optics letters*, 28(8):607–9, April 2003.

[9] Hongping Ding, Qinghui Li, and Wenyi Zou. Design and comparison of amplitude-type and phase-only transverse super-resolving pupil filters. *Optics Communications*, 229(1-6):117–122, January 2004.

[10] Fang Huang, Samantha L Schwartz, Jason M Byars, and Keith a Lidke. Simultaneous multiple-emitter fitting for single molecule super-resolution imaging. *Biomedical optics express*, 2(5):1377–93, January 2011.

[11] Zbigniew Jaroszewicz, Anna Burvall, and Ari T. Friberg. Axicon - the Most Important Optical Element. *Optics and Photonics News*, 16(4):34, 2005.

[12] Hong Jin, Daniel a Heller, and Michael S Strano. Single-particle tracking of endocytosis and exocytosis of single-walled carbon nanotubes in NIH-3T3 cells. *Nano letters*, 8(6):1577–85, June 2008.

[13] Christian J. Kähler, Sven Scharnowski, and Christian Cierpka. On the resolution limit of digital particle image velocimetry. *Experiments in Fluids*, February 2012.

[14] Joseph Katz and Jian Sheng. Applications of Holography in Fluid Mechanics and Particle Dynamics. *Annual Review of Fluid Mechanics*, 42(1):531–555, January 2010.

[15] Seok Kim and Sang Joon Lee. Measurement of 3D laminar flow inside a micro tube using micro digital holographic particle tracking velocimetry. *Journal of Micromechanics and Microengineering*, 17(10):2157–2162, October 2007.

[16] Aloke Kumar, Christian Cierpka, Stuart J. Williams, Christian J. Kähler, and Steven T. Wereley. 3D3C velocimetry measurements of an electrothermal microvortex using wavefront deformation PTV and a single camera. *Microfluidics and Nanofluidics*, 10(2):355–365, July 2010.

[17] Ralph Lindken, Massimiliano Rossi, Sebastian Groß e, and Jerry Westerweel. Micro-Particle Image Velocimetry (PIV): Recent developments, applications, and guidelines. *Lab on a Chip*, 9(17):2551, 2009.

[18] Jian Lu, Francisco Pereira, Scott E Fraser, and Morteza Gharib. Three-dimensional real-time imaging of cardiac cell motions in living embryos. *Journal of biomedical optics*, 13(1):14006, 2012.

[19] John H McLeod. The Axicon: A New Type of Optical Element. *Journal of the Optical Society of America*, 44(8):592, August 1954.

[20] C. D. Meinhart, S. T. Wereley, and J. G. Santiago. PIV measurements of a microchannel flow. *Experiments in Fluids*, 27(5):414–419, October 1999.

[21] M a Neil, R Juskaitis, T Wilson, Z J Laczik, and V Sarafis. Optimized pupil-plane filters for confocal microscope point-spread function engineering. *Optics letters*, 25(4):245–247, February 2000.

[22] M. G. Olsen and R. J. Adrian. Out-of-focus effects on particle image visibility and correlation in microscopic particle image velocimetry. *Experiments in Fluids*, 29(7):S166–S174, December 2000.

[23] Michael J Rust, Mark Bates, and Xiaowei Zhuang. Sub-diffraction-limit imaging by stochastic optical reconstruction microscopy (STORM). *Nature methods*, 3(10):793–5, October 2006.

[24] T R Sales and G M Morris. Fundamental limits of optical superresolution. *Optics letters*, 22(9):582–4, May 1997.

[25] J. G. Santiago, S. T. Wereley, C. D. Meinhart, D. J. Beebe, and R. J. Adrian. A particle image velocimetry system for microfluidics. *Experiments in Fluids*, 25(4):316–319, September 1998.

[26] Shin-ichi Satake, Tomoaki Kunugi, Kazuho Sato, Tomoyoshi Ito, Hiroyuki Kanamori, and Jun Taniguchi. Measurements of 3D flow in a micro-pipe via micro digital holographic particle tracking velocimetry. *Measurement Science and Technology*, 17(7):1647–1651, July 2006.

[27] Jian Sheng, Edwin Malkiel, and Joseph Katz. Digital holographic microscope for measuring three-dimensional particle distributions and motions. *Applied Optics*, 45(16):3893, 2006.

[28] Craig Snoeyink and Steve Wereley. Three-dimensional locating of paraxial point source with axicon. *Optics Letters*, 37(11):2058, May 2012.

[29] Craig Snoeyink and Steve Wereley. A novel 3D3C particle tracking method suitable for microfluidic flow measurements. *Experiments in Fluids*, 54(1):1453, January 2013.

[30] Craig Snoeyink and Steve Wereley. Single-image far-field subdiffraction limit imaging with axicon. *Optics Letters*, 38(5):625, February 2013.

[31] Myong Hwan Sohn, Kyung Won Seo, Yong Seok Choi, Sang Joon Lee, Young Sil Kang, and Yang Soon Kang. Determination of the swimming trajectory and speed of chain-forming dinoflagellate Cochlodinium polykrikoides with digital holographic particle tracking velocimetry. *Marine Biology*, 158(3):561–570, November 2010.

[32] Michael Speidel, Alexandr Jonás, and Ernst-Ludwig Florin. Three-dimensional tracking of fluorescent nanoparticles with subnanometer precision by use of off-focus imaging. *Optics letters*, 28(2):69–71, January 2003.

[33] Wei-Hsin Tien, Patrick Kartes, Toru Yamasaki, and Dana Dabiri. A color-coded backlighted defocusing digital particle image velocimetry system. *Experiments in Fluids*, 44(6):1015–1026, January 2008.

[34] Arnold Vainrub, Oleg Pustovyy, and Vitaly Vodyanoy. Resolution of 90 nm (λ/5) in an optical transmission microscope with an annular condenser. *Optics Letters*, 31(19):2855, 2006.

[35] Steven T. Wereley and Carl D. Meinhart. Recent Advances in Micro-Particle Image Velocimetry. *Annual Review of Fluid Mechanics*, 42(1):557–576, 2010.

[36] C E Willert and M Gharib. Three-dimensional particle imaging with a single camera. *Experiments in Fluids*, 12(6), April 1992.

[37] Denis Wirtz. Particle-tracking microrheology of living cells: principles and applications. *Annual review of biophysics*, 38:301–26, January 2009.

[38] Mingming Wu, John W. Roberts, and Mark Buckley. Three-dimensional fluorescent particle tracking at micron-scale using a single camera. *Experiments in Fluids*, 38(4):461–465, February 2005.

[39] S Y Yoon and K C Kim. 3D particle position and 3D velocity field measurement in a microvolume via the defocusing concept. *Measurement Science & Technology*, 17(11):2897–2905, November 2006.